CHAPTER 3

Hydration Dynamics at Fluorinated Protein Surfaces

Portions of this chapter are adapted from a paper in preparation by Tae Hyeon Yoo, Oh-Hoon Kwon, David A. Tirrell, and Ahmed H. Zewail.

Abstract

We report here studies of local hydration dynamics at fluorinated protein surfaces. 5,5,5-Trifluoroleucine (Tfl) was incorporated into the Leu positions of three coiled-coil proteins, and the time-dependent fluorescence Stokes shift of a single solvent-exposed Trp residue was monitored with femtosecond resolution. While fluorination of the hydrophobic core did not change the rate of solvent reorganization following excitation of Trp, introduction of Tfl adjacent to the chromophore slowed the hydration dynamics. The results suggest that the dipole moment of the trifluoromethyl group plays an important role in modulating hydration dynamics at the protein surface, and provide new insight into the origin of the hydrophobic character of fluorinated amino acid side chains.

Introduction

The past decade has seen substantial expansion in the number and diversity of noncanonical amino acids that can be incorporated into recombinant proteins.[1] Among the various analogues, fluorinated amino acids have drawn attention due to the possibility of creating novel biological molecules.[2-6] For example, several independent studies have shown that fluorination of the hydrophobic core of coiled-coil proteins through incorporation of fluorinated amino acids can improve their stability by virtue of the

hyper-hydrophobicity (and fluorophilicity) of fluorinated compounds.[3] However, the C-F bond has several unique properties different from C-H bonds.[7] The C-F bond has a strong dipole moment due to the electronegativity of fluorine, and the dipolar bond is relatively nonpolarizable. The C-F bond can exert a strong inductive effect on neighboring bonds and interact with ionic or dipolar groups by electrostatic (dipole-dipole or point-dipole) interactions in appropriately organized systems. The strong dipole moment of the C-F bond with its hydrophobicity has been referred to as "polar hydrophobicity," and plays an important role in organic and medicinal chemistry. In addition, the C-F bond is significantly longer than a C-H bond, and the calculated volume of the trifluoromethyl group is about twice as large as that of a methyl group and similar to that of an ethyl group.

The hydration layer around protein surfaces exhibits properties different from those of bulk water; the more rigid and denser structure of the hydration layer plays a crucial role in protein structure, folding, dynamics, and function.[8-10] The elucidation of the dynamic features of this region on the time scales of atomic and molecular motion is essential in understanding the nature of protein hydration. Recently, the dynamic properties of the hydration layer have been extensively studied for various proteins using Trp as a local fluorescent probe or using synthetic fluorescent amino acids, and the

results have revealed multicomponent relaxation dynamics on a wide range of time scales. [10-12] The initial relaxation occurs in a few hundred femtoseconds (fs) to a few ps depending on exposure of the Trp residue to water, and is attributed to fast librational/rotational dynamics of water molecules. The slow relaxation dynamics, which spans from a few tens of ps to hundreds of ps, was initially assigned to the exchange dynamics between free and bound water at the vicinity of biological surfaces.[10] Recently, the idea of coupled water-protein fluctuation was introduced to account for the slow hydration dynamics. [11g, 13-15]

The nature of the protein hydration layer can be affected not only by the topological and electrostatic properties of the protein surfaces,[9] but also by the physical and chemical properties of individual surface-exposed residues.[11g,16] Considering the unique properties of the C-F bond, the interactions of fluorinated compounds with water molecules could be different from those of polar or hydrophobic molecules. In this paper, we report studies of the local hydration dynamics at fluorinated protein surfaces by monitoring the time-dependent fluorescence Stokes shift of Trp residues located at a surface-exposed position of coiled-coil proteins carrying 5,5,5-trifluoroleucine (Tfl) residues adjacent to the probe.

Results and Discussion

The coiled-coil protein A1 (Fig. 3.1) was used as a model system to examine the effects of fluorinated amino acids on local hydration dynamics. The primary structure of A1 consists of copies of a heptad repeat $(abcdefg)_n$, where positions *a* and *d* are occupied by hydrophobic amino acids. Self-association of the peptide juxtaposes the *a* and *d* positions and forms a hydrophobic core. Previously, fluorinated leucine (Leu) analogues were incorporated into the *d* positions of A1; the fluorinated proteins exhibited improved resistance to thermal and chemical denaturation with minimal differences in secondary structure.[3a,b] In this work, the surface-exposed Asp residue at the *f* position of the third heptad was replaced by Trp, which serves as a fluorescence probe (Fig. 3.1B). In order to examine the effects of fluorinated analogues on the local hydration dynamics, a Leu codon was introduced at the *c* position of the third heptad to yield S31L or at the *b* position of the fourth heptad to yield A37L.

The three A1 variants (A1m, S31L, and A37L) were expressed in 2xYT medium to yield proteins A1m-L, S31L-L, and A37L-L, respectively, or in M9 minimal medium supplemented with 19 amino acids plus Tfl to give A1m-T, S31L-T, and S37L-T. The proteins were purified under denaturing conditions and dialyzed against 10 mM acetate

(pH 4)/100 mM NaCl solution. The extent of replacement of Leu by Tfl in each protein was determined by amino acid analysis to be 90-91%.

Circular dichroism spectroscopy indicated that all six proteins were helical, as determined from the molar ellipticity at 222 nm (Fig. 3.2);[17] the overlap of the spectra suggests nearly identical secondary structures. The oligomerization states of the protein samples were determined by sedimentation velocity analysis (Fig. 3.3). Although A1 forms dimers and tetramers at neutral pH,[3a] the variants examined in this study form trimers or hexamers under mildly acidic conditions (pH 4). Protonation of the Glu residues at the *e* and *g* positions of the proteins decreases the density of negative charges adjacent to the hydrophobic core, and seems to promote formation of the trimers or hexamers rather than dimers or tetramers. A1m, in which one Trp residue occupies a surface-exposed position, is predominantly trimers in both the Leu- and Tfl-forms, with a small portion of hexamers (Fig. 3.3 A and B). However, the majority of S31L is present as hexamers (Fig. 3.3 C and D). Interestingly, while A37L-L seems to be a mixture of trimers, tetramers, pentamers, and hexamers, as indicated by the broad distribution of its sedimentation coefficient, A37L-T is a mixture of trimers and hexamers (Fig. 3.3 E and F). We suspect that the incomplete replacement of Leu with Tfl caused the broader distribution of the Tfl-form proteins.

The steady-state fluorescence emission spectrum of Trp depends the extent of exposure to water.[18] All six protein samples showed emission maxima at 349-352 nm, close to that of free Trp (Table 3.1). This observation indicates that the Trp residues are exposed to the aqueous environment (consistent with the original design), and not involved in oligomerization of the proteins. Each pair of Leu- and Tfl-form proteins showed very similar emission maxima within 1 nm. The absorption spectra of the proteins are nearly the same as that of free Trp (data not shown).

The mobility of the probe residue was explored in each protein by measuring fs-resolved depolarization dynamics (Fig. 3.4). The anisotropic dynamics was found to consist of three components: ultrafast (≤ 500 fs), fast (~ 100 ps), and slow (> 500 ps) decays (Table 1). The ultrafast decays are attributed to fast internal conversion between the first two singlet excited states (^1L_a and ^1L_b) of Trp; the fast decays to local wobbling motions; the slow decays to tumbling motions of proteins.[11f] The introduction of Leu adjacent to the Trp probe resulted in faster Trp rotational motions (ϕ_{Trp}, Table 3.1) with smaller wobbling con semiangles (θ, Table 3.1). However, relatively similar values were observed in Trp-rotational anisotropic dynamics for each pair of Leu- and Tfl-proteins.

Mutation of residues around Trp is expected to affect the environment of the probe and thus to result in changes of thermodynamic or/and dynamic properties of the

hydration layer. In many cases these properties are related to one another. However, dynamic properties can be changed without any effect on thermodynamics because thermodynamics depends only on equilibrium states. The observed minimal effects of replacement of Leu by Tfl on the steady-state fluorescence emission suggest similar thermodynamic features of the hydration region. In addition, the similarity of the Trp wobbling motions of the Leu- and Tfl-forms of the proteins suggests similar organization of neighboring residues around the probe. Moreover, this excludes possibilities that the motions affect the hydration dynamics differently, even though the time scales for the Trp wobbling motions are slower than those of the hydration dynamics as described later (Table 3.1 and Fig. 3.6). All these features make it possible to compare the dynamic properties of protein hydration for each pair of Leu- and Tfl-form proteins.

To investigate the ultrafast hydration dynamics at the protein surfaces, we utilized a methodology recently developed by Zhong and coworkers for the reconstruction of fs-resolved fluorescence spectra.[11f,19] As an example, Fig. 3.5A shows several representative fs-resolved fluorescence transients of A1m-T. The overall decay dynamics is retarded compared with that of free Trp in the buffer solution. Besides the lifetime components of 0.26, 1.6, and 5.5 ns, which were obtained by global analysis of fluorescence transients collected using a time-correlated single photon counting

spectrometer, all transients show additional multiple exponential decay (at the blue side) and rise (at the red side) with time constants spanning from a few hundred fs to several tens of ps. The existence of multiple Trp conformers, each of which has a distinctive fluorescence spectrum and lifetime, can cause time-dependent spectral shift as well. In order to extract hydration dynamics precisely, we reconstructed apparent and lifetime-associated fs-resolved fluorescence spectra with eight or nine transients at different wavelengths covering the blue and the red sides (Fig. 3.5B). By fitting these spectra to lognormal functions, we traced the time-dependent apparent emission maxima (ν_s) and lifetime-associated emission maxima (ν_l) as plotted in Fig. 5C. Using $\Delta\nu(t) = \nu_s(t) - \nu_l(t)$, we correlated the extracted time-dependent spectral shift, $\Delta\nu(t)$, to the hydration energy relaxation, ΔE_s (Fig. 3.6). Details of the results for all protein samples are presented in Table 3.1.

Several key features of the results (Fig. 3.6 and Table 3.1) are summarized as follows. First, the hydration dynamics of the proteins were well represented by triple exponential decays with distinctive time scales of 0.28-0.79, 1.7-6.1, and 13-61 ps. Relaxation occurring on a timescale of a few hundred fs to several ps is attributed to fast librational/rotational motions of bulk type water molecules around Trp. Of note is that the local hydration dynamics around Trp that is crowded by nearby residues and partially

exposed to water is reported to lack the fs component.[11f,g,14] Second, A1m-L and A1m-T, which differ only in the nature of the hydrophobic core, exhibited almost identical hydration dynamics. The slowest phase of hydration dynamics on the time scale of tens of ps is coupled to protein fluctuation dynamics,[11g,13-15] and it has been shown that fluorination of the hydrophobic core of a helix bundle protein can affect protein dynamics.[20] However, the nearly identical hydration dynamics for A1m-L and A1m-T up to a few hundred ps implies that fluorination of the hydrophobic core does not affect the protein motions that can be coupled with the local hydration dynamics on the time scale of our interest. Third, S31L-T and A37L-T, in which Tfl lies close to Trp as well as in the hydrophobic core, showed slower hydration dynamics than their Leu counterparts, indicating that the fluorinated surface of the protein retards the hydration dynamics.

Computational studies have shown that the hydration interface of a large hydrophobic surface with low curvature has depleted-water layers different from a wet surface around small hydrophobic and hydrophilic hydrophilic molecules,[21] and this region has been proposed to be similar to a liquid-vapor interface.[21,22] The density of water molecules is fluctuating rather than static,[21,23] and the properties of the interface are affected by the interactions between the surface and water, such as van der Waals attractions.[21,24] Recently, molecular dynamics simulation studies have shown that a

folded β-hairpin peptide has lower hydration density around its hydrophobic residues than its hydrophilic ones.[16] In addition, Qiu et al. showed that mutation of charged or polar residues of the enzyme staphylococcal nuclease into a more hydrophobic one (Ala) resulted in faster hydration dynamics, which was attributed to strong interaction between the charges (or dipoles) and water molecules.[11g] In addition, Head-Gordon and coworkers have reported heterogeneous water dynamics in the first hydration shell of model peptides (*N*-acetyl-leucine-methylamide and *N*-acetyl-glycine-methylamide), with faster water motions near the hydrophobic side chain and much slower water motion near the hydrophilic backbone.[25] These observations suggest that water molecules neighboring hydrophobic side chains in the hydration layer of proteins have similar properties to those at extended hydrophobic surfaces rather than those around small hydrophobic molecules.

In this study, the effects of fluorinated amino acids on the local hydration were examined by installing Tfl near the Trp residue of the model protein. Even though Tfl is more hydrophobic than Leu, the neighboring Tfl residue caused the retardation of the local hydration dynamics (Fig. 3.6 and Table 3.1). The hydration dynamics around fluorinated compounds cannot be explained only by their hydrophobic properties. Although the C-F bond has been assumed not to be involved in hydrogen bonding with

liquid water,[2c] the strong dipole moment of the C-F bond exerts stronger interactions on water molecules compared to C-H bonds, and might induce a more organized structure of water molecules. As a result, the water molecules around the trifluoromethyl group are involved in the relaxation process on a slower time scale.

The hydrophobicity of a compound can be quantified in terms of a free energy change for solvent to reorganize and solvate the solute, which has two primary components of enthalpic and entropic changes. Fluorinated compounds have higher hydrophobicity than hydrogenated ones.[2,7] Because the van der Waals radius of a C-F bond is larger than that of a C-H bond, the more hydrophobic properties can be thought to just come from the size difference.[7d] In the case of fluorinated compounds, however, there are favorable enthalpic contributions on solvation coming from the electrostatic interactions between water molecules and the polar C-F bond and should be more entropic penalty, suggesting more ordered structure of water molecules at the hydration interface compared to hydrogenated compounds.

The study reported here showed that fluorinated amino acids influence hydration dynamics in a manner quite different from that of their hydrogenated counterparts. The strong dipole moment of the C-F bond explains the retarded hydration dynamics. These results point to the importance of the polar hydrophobic property of the C-F bond in

understanding the interactions of fluorinated compounds with others or themselves, and give new insight in understanding the hyper-hydrophobic character of fluorinated amino acid side chains.

Materials and Methods

Materials. All restriction enzymes were purchased from New England Biolabs (Beverly, MA). 5,5,5-trifluoroleucine (Tfl) was purchased from Oakwood Products (West Columbia, SC). DNA oligomers were synthesized at Qiagen (Valencia, CA).

Plasmid construction. An *Eco*RI/*Hin*dIII fragment of pQEA1[3a] containing the A1 coding sequence was ligated into *Eco*RI/*Hin*dIII-digested pQE-80L (Qiagen) to yield pQE-80L/A1. The Asp residue at position 34 of A1 was changed Trp by site-directed mutagenesis. The resulting plasmid was designated pQE-80L/A1m. A Leu codon was introduced into either at position 31 or at position 37, yielding pQE-80L/S31L and pQE-80L/A37L, respectively.

Expression of fluorinated proteins. M9 medium supplemented with 0.4% glucose, 3.5 mg/L thiamine, 1 mM $MgSO_4$, 0.1 mM $CaCl_2$, 20 amino acids (40 mg/L), 200 mg/L

ampicillin was inoculated 1/50 with an overnight culture (M9) of *E. coli* strain DH10B transformed with pQE-80L/A1m, pQE-80L/S31L, or pQE-80L/A37L. After each culture reached OD_{600} = 0.9 – 1.0, the cells were harvested by centrifugation (6,000×g, 4 °C, 6 min) and washed twice with cold 0.9 % NaCl. The cell pellets were resuspended in supplemented M9 medium containing 19 amino acids (no Leu) and 1 mM Tfl. Protein expression was induced 10 min after the medium shift by addition of isopropyl-β-D-thiogalactoside (IPTG) to a final concentration of 1 mM. After 3 h, the cells were harvested by centrifugation (6,000×g, 4 °C, 10 min), and the cells were stored at -20^{o}C at least 12 h before purification.

Expression of hydrogenated proteins. 2xYT medium was used instead of supplemented M9 medium. When the culture reached OD_{600} = 0.9 – 1.0, IPTG was added to a final concentration of 1 mM. After 3 h, the cells were harvested by centrifugation (6,000×g, 4 °C, 10 min), and the cells were stored at -20^{o}C at least 12 h before purification.

Protein purification. N-terminally histidine-tagged A1 variants were purified under denaturing conditions by affinity chromatography using Ni-NTA resin (Qiage, Chatsworth, CA) according to the manufacturer's instructions. The purified protein

solutions were dialyzed against 10 mM sodium acetate (pH 4)/100 mM NaCl, and were concentrated by ultrafiltration (Amicon Ultra, mwco: 10,000, Millipore, Billerica, MA). The protein concentration was determined as measured by the absorbance at 280 nm of solutions, assuming extinction coefficients 5500 $M^{-1}cm^{-1}$.[26]

Amino acid analysis, circular dichroism spectroscopy, steady-state fluorescence, and sedimentation velocity analysis. Amino acid analysis was performed at the W. M. Keck Facility at Yale University (New Haven, CT) on a Hitachi L-8900 amino acid analyzer (San Jose, CA) after hydrolysis at 115 ^{o}C in 70 % formic acid. Circular dichroism spectra were recorded on an Aviv 62DS spectropolarimeter (Lakewood, NJ). Steady-state fluorescence emission spectra were measured using a FluoroMax-2 fluorimeter (ISA-Spex). Sedimentation velocity analysis was performed at the National Analytical Ultracentrifugation Facility at the University of Connecticut (Storrs, CT) by using a Beckman XL-I Analytical Ultracentrifuge at 20^{o}C. The rotor was accelerated to 55,000 rpm, and interference scans were acquired at one minute intervals for 7 h. The data were analyzed by using the program Sedfit[27] to obtain normalized c(s) versus sedimentation coefficient plots.

Time-correlated single-photon Counting (TCSPC). The protein samples were prepared at 55 μM concentration in 10 mM acetate (pH 4)/100 mM NaCl solution. The TCSPC measurements were performed by using femtosecond pulses (<100 fs) from a Ti-sapphire oscillator (Spectra-Physics, Mai Tai HP). Laser output, of which repetition rate was attenuated from 80 MHz to 8 MHz with utilizing a pulse picker (Spectra-Physics, Model 3980-5), was tuned to 885 nm and frequency-tripled to 295 nm using a time-plate tripler (Minioptic Technology, TP-2000B) for selective excitation of Trp. The vertically polarized UV beam using a half waveplate was introduced to a sample chamber and focused onto the sample cell. The residual frequency-doubled beam from the tripler was directed to a photodiode to trigger a TCSPC system (PicoQuant GmbH, FluoTime 200). Typically, the energy of the excitation pulse (attenuated) at the sample was ~10 pJ. In a right-angle geometry, the emitted fluorescence was collected at a magic angle (54.7^{o}) with respect to the vertically polarized excitation beam and focused into a MCP-PMT (Hamamatsu, R3809U), which is attached to a double monochromator. The PMT signal was routed to a time-to-amplitude converter as a start signal followed by a constant fractional discriminator (PicoQuant GmbH, SPC 630). To avoid possible photobleaching and photodegradation, samples were kept stirring using a micro magnetic stirrer. In this configuration, the instrument response has a full width at half maximum of ~30 ps.

Multiexponential decays convoluted with instrumental response functions were analyzed using the FluoFit software package (PicoQuant).

Femtosecond fluorescence upconversion. The protein samples were prepared at 550 μM concentration in 10 mM acetate (pH 4)/100 mM NaCl solution. We used an amplified Ti-sapphire laser system (Spectra-Physics, Hurricane X), which produces ~110-fs pulses centered at 805 nm (fundamental), with a 1-kHz repetition rate and a 0.8-mJ energy. The output beam was split into equal parts to generate the pump and the gate pulse trains. For the pump, the fundamental light was used to pump an optical parametric amplifier (Spectra-Physics, OPA-800C), the IR idler output of which was sum-frequency mixed with the residual fundamental in a 0.5-mm thick β-barium borate (BBO) crystal (type I), recompressed with a prism pair, and frequency-doubled to provide the 295-nm pulses in a 1.0-mm thick BBO crystal. The pump pulses were focused, by a lens having the focal length of 24 cm, on the rotating circular cell (1-mm thickness) containing the sample. Typically, the energy of the pump pulse (attenuated) at the sample was ~200 nJ. At these energies, the fluorescence signals from samples were linearly dependent on the pump energy. To check for sample degradation during experiments, fluorescence spectra were periodically measured right after the rotating cell by using a fiber-optic-coupled

spectrometer (Acton Research, SpectraPro-300i) coupled to a CCD (Princeton Instruments, SpectruMM-256HB) before and after the collection of averaged transients for each sample. No difference between the spectra was observed.

The forward-scattered fluorescence from excited samples was collected and focused by two off-axis parabolic mirrors into a 0.5-mm thick BBO crystal. Cutoff filters were placed between the mirrors to reject scattered laser light and pass the desired fluorescence wavelengths. The gate pulses, attenuated to 23 μJ/pulse, passed through a computer-controlled optical delay line and were noncollinearly overlapped with the fluorescence in the BBO crystal. After the crystal, the upconverted signal was separated from the gate beam and the fluorescence by using an iris, and was focused on the entrance slit of a 0.25-m double-grating monochromator (Jobin Yvon, DH10) equipped with a photomultiplier tube at the exit slit. Upconversion efficiency was maximized by angle-tuning of the BBO crystal. The upconverted fluorescence transients were taken at the magic angle (54.7^{o}) of the pump polarization relative to the gate polarization, parallel to the acceptance axis of the upconversion crystal, in order to eliminate the influence of induced sample anisotropy on the signal. The photomultiplier output was amplified (SRS, SR445) and processed by a gated integrator (SRS, SR250). The temporal response of the instrument was typically 500 fs. The observed fluorescence transients were fit to

theoretical functions, using a Scientist nonlinear least-squares fitting program (Micromath), for the convolution of the Gaussian instrument response function with a sum of exponentials. All experiments were carried out at an ambient temperature of ~24 ^{o}C, and all fluorescence transients were obtained by the excitation of samples at 295 nm.

For fluorescence anisotropy measurements, the pump-beam polarization was rotated either parallel or perpendicular to the acceptance axis of the upconversion crystal to collect the parallel ($I_{\parallel}$) and perpendicular ($I_{\perp}$) signals, respectively. These transients were used to construct time-resolved anisotropy: $r(t) = (I_{\parallel} - I_{\perp})/(I_{\parallel} + 2I_{\perp})$.

References

[1] a) A. J. Link, M. L. Mock, D. A. Tirrell, *Curr. Opin. Biotechnol.* **2003**, *14*, 603-609; b) J. Xie, P. G. Schultz, *Nat. Rev. Mol. Cell Biol.* **2006**, *7*, 775-782; c) N. Budisa, *Angew. Chem.* **2004**, *116*, 6586-6624; *Angew. Chem. Int. Ed.* **2004**, *43*, 6426-6463.

[2] a) E. N. Marsh, *Chem. Biol.* **2000**. *7*, R153-R157; b) N. C. Yoder, K. Kumar, *Chem. Soc. Rev.* **2002**, *3*, 335-341.

[3] a) Y. Tang, G. Ghirlanda, W. A. Petka, T. Nakajima, W. F. DeGrado, D. A. Tirrell, *Angew. Chem.* **2001**, *113*, 1542-1544; *Angew. Chem. Int. Ed.* **2001**, *40*,1494-1496; b) Y. Tang, D. A. Tirrell, *J. Am Chem. Soc.* **2001**, *123*, 11089-11090; c) S. Son, I. C. Tanrikulu,

D. A. Tirrell, *ChemBioChem* **2006**, *7*, 1251-1257; d) K.-H. Lee, H.-Y. Lee, M. M. Slutsky, J. T. Anderson, E. N. G. Marsh, *Biochemistry* **2004**, 43, 16277-16284; e) B. Bilgiçer, B. A. Fichera, K. Kumar, *J. Am. Chem. Soc.* **2001**, *123*, 4393-4399; g) C. Jäckel, M. Salwiczek, B. Koksch, *Angew. Chem.* **2006**, *118*, 4305-4309; *Angew. Chem. Int. Ed.* **2006**, *45*, 4198-4203.

[4] a) A. Niemz, D. A. Tirrell, *J. Am. Chem. Soc.* **2001**, *123*, 7407-7413; b) B. Bilgiçer, K. Kumar, *Proc. Natl. Acad. Sci. USA* **2004**, *101*, 5324-15329; c) J.-C. Horng, D. P. Raleigh, *J. Am. Chem. Soc.* **2003**, *125*, 9286-9287.

[5] a) M. D. Vaughan, P. Cleve, V. Robinson, H. S. Duewel, J. F. Honek, *J. Am. Chem. Soc.* **1999**, *121*, 8475-8478; b) J. G. Bann, J. Pinkner, S. J. Hultgren, C. Frieden, *Pro. Natl. Acad. Sci. USA* **2002**, *99*, 709-714; c) J. C. Jackson, J. T. Hammill, R. A. Mehl, *J. Am. Chem. Soc.* **2007**, *129*, 1160-1166.

[6] a) P. Wang, Y. Tang, D. A. Tirrell, *J. Am. Chem. Soc.* **2003**, *125*, 6900-6906; b) J. K. Montclare, D. A. Tirrell, *Angew. Chem*. **2006**, *118*, 4630-4633; *Angew. Chem. Int. Ed.* **2006**, *45*, 4518-4521; c) T. H. Yoo, A. J. Link, D. A. Tirrell, *Pros. Natl. Acad. Sci. USA* **2007**, *104*, 13887-13890; d) T. H. Yoo, D. A. Tirrell, *Angew. Chem*. **2007**, *119*, 5436-5439; *Angew. Chem. Int. Ed.* **2007**, *46*, 5340-5343.

[7] a) J. C. Biffinger, H. W. Kim, S. G. DiMagno, *ChemBioChem* **2004**, *5*, 622-627; b) K. Müller, C. Faeh, F. Diederich, *Science* **2007**, *317*, 1881-1886; c) F. Leroux, *ChemBioChem* **2004**, *5*, 644-649; d) J. Gao, S. Qiao, G. M. Whitesides, *J. Med. Chem.* **1995**, *38*, 2292-2301; e) C. Jäckel, B. Koksch, *Eur. J. Org. Chem.* **2005**, 4483-4503.

[8] a) D. I. Svergun, S. Richard, M. H. J. Koch, Z. Sayers, S. Kuprin, G. Zaccai, *Proc. Natl. Acad. Sci. USA* **1998**, *95*, 2267-2272.

[9] a) Y.-K. Cheng, P. J. Rossky, *Nature* **1998**, *392*, 696-699; b) F. Merzel, J. C. Smith, *Proc. Natl. Acad. Sci. USA* **2002**, *99*, 5378-5383.

[10] a) S. K. Pal, A. H. Zewail, *Chem. Rev.* **2004**, *104*, 2099-2123; b) S. K. Pal, J. Peon, B. Bagchi, A. H. Zewail, *J. Phys. Chem. B* **2002**, *106*, 12376-12395.

[11] a) S. K. Pal, J. Peon, A. H. Zewail, *Proc. Natl. Acad. Sci. USA* **2002**, *99*, 1763-1768; b) J. Peon, S. K. Pal, A. H. Zewail, *Proc. Natl. Acad. Sci. USA* **2002**, *99*, 10964-10969; c) L. Zhao, S. K. Pal, T. Xia, A. H. Zewail, *Angew. Chem. Int. Ed.* **2004**, *43*, 60-63; d) S. K. Pal, J. Peon, A. H. Zewail, *Proc. Natl. Acad. Sci. USA* **2002**, *99*, 15297-15302; e) J. K. A. Kamal, L. Zhao, A. H. Zewail, *Proc. Natl. Acad. Sci. USA* **2004**, *101*, 13411-13416; f) W. Qiu, L. Zhang, O. Okobiah, Y. Yang, L. Wang, D. Zhong, A. H. Zewail, *J. Phys. Chem. B* **2006**, *110*, 10540-10549; g) W. Qiu, Y.-T. Kao, L. Zhang, Y. Yang, L. Wang, W. E. Stites, D. Zhong, A. H. Zewail, *Proc. Natl. Acad. Sci. USA* **2006**, *103*, 13979-13984.

[12] a) B. E. Cohen, T. B. McAnaney, E. S. Park, Y. N. Jan, S. G. Boxer, L. Y. Jan, *Science* **2002**, *296*, 1700-1703; b) P. Abbyad, X. Shi, W. Childs, T. B. McAnaney, B. E. Cohen, S. G. Boxer, *J. Phys. Chem. B* **2007**, *111*, 8269-8276.

[13] A. A. Golosov, M. Karplus, *J. Phys. Chem. B* **2007**, *111*, 1482-1490.

[14] T. Li, A. A. Hassanali, Y.-T. Kao, D. Zhong, S. J. Singer, *J. Am. Chem. Soc.* **2007**, *129*, 3376-3382.

[15] W. Qiu, L. Wang, W. Lu, A. Boechler, D. A. R. Sanders, D. Zhong, *Proc. Natl. Acad. Sci. USA* **2007**, *104*, 5366-5371.

[16] I. Daidone, M. B. Ulmschneider, A. Di Nola, A. Amadei, J. C. Smith, *Proc. Natl. Acad. Sci. USA* **2007**, *104*, 15230-15235.

[17] Y.-H. Chen, J. T. Yang, H. M. Martinez, *Biochemistry* **1972**, *11*, 4120-4131.

[18] J. T. Vivian, P. R. Callis, *Biophys. J.* **2001**, *80*, 2093-2109.

[19] W. Lu, J. Kim, W. Qiu, D. Zhong, *Chem. Phys. Lett.* **2004**, *388*, 120-126.

[20] H.-Y. Lee, K.-H. Lee, H. M. Al-Hashimi, E. N. G. Marsh, *J. Am. Chem. Soc.* **2005**, *128*, 337-343.

[21] D. Chandler, *Nature* **2005**, *437*, 640-647.

[22] a) G. L. Richmond, *Chem. Rev.* **2002**, *102*, 2693-2724; b)Y. R. Shen, V. Ostroverkhov, *Chem. Rev.* **2006**, *106*, 1140-1154.

[23] a) P. R. ten Wolde, D. Chandler, *Proc. Natl. Acad. Sci. USA* **2002**, *99*, 6539-6543; b) T. F. Miller III, E. Vanden-Eijnden, D. Chandler, *Proc. Natl. Acad. Sci. USA* **2007**, *104*, 14559-14564.

[24] a) H. S. Ashbaugh, M. F. Paulaitis, *J. Am. Chem. Soc.* **2001**, *123*, 10721-10728; b) D. M. Huang, D. Chandler, *J. Phys. Chem. B* **2002**, *106*, 2047-2053;c) T. R. Jensen, M. Ø. Jensen, N. Reitzel, K. Balashev, G. H. Peters, K. Kjaer, T. Bjørnholm, *Phy. Rev. Lett.* **2003**, *90*, 086101.1-086101.4.

[25] a) D. Russo, G. Hura, T. Head-Gordon, *Biophys. J.* **2004**, *86*, 1852-1862; b) D. Russo, R. K. Murarka, J. R. D. Copley, T. Head-Gordon, *J. Phys. Chem. B* **2005**, *109*, 12966-12975.

[26] ProtParam Software can be found under http://ca.expasy.org/tools/protparam.html.

[27] P. Schuck, *Biophys. J.* **2000**, *78*, 1606-1619.

Fig. 3.1. A) Helical wheel diagram of a coiled-coil protein. B) Amino acid sequence of A1. Heptad repeats are designated by italic letters, *abcdefg*.

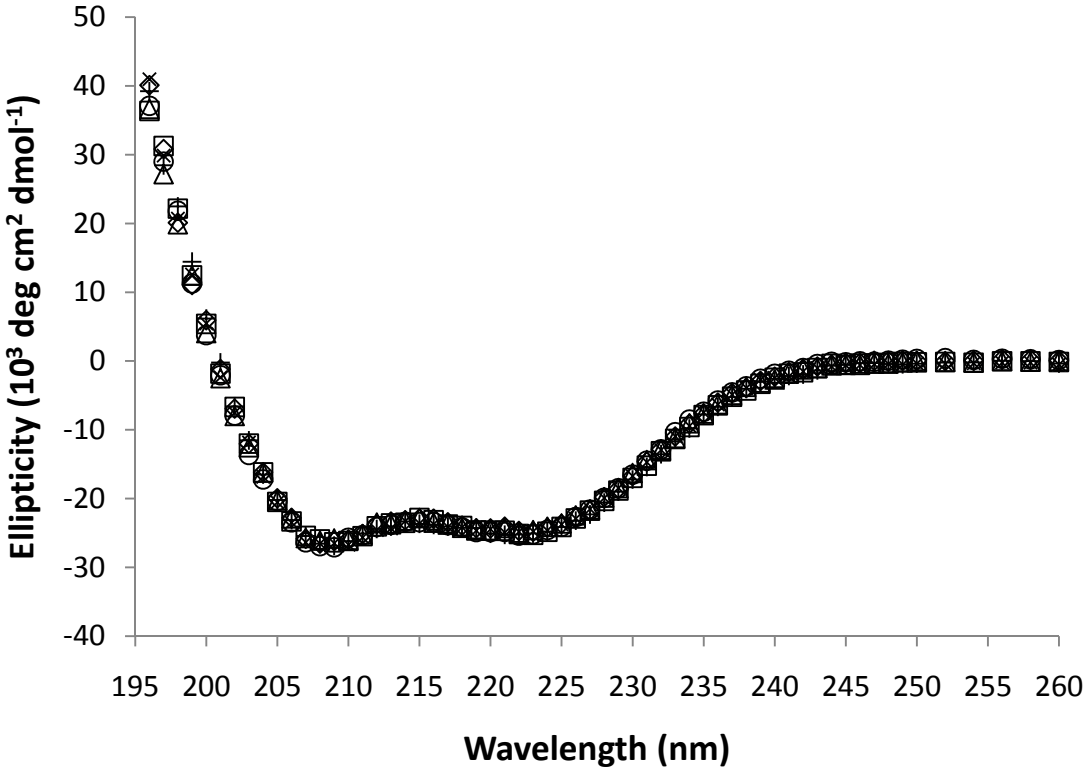

Fig. 3.2. Circular dichroism spectra of A1m-L (◊), and Alm-T (○), S31L-L (+), S31L-T (×), A37L-L (□), A37L-T (Δ) at 25 ºC. The protein samples were prepared at 20 μM concentration in 10 mM acetate (pH 4)/100 mM NaCl solution.

Fig. 3.3. Normalized plots from the Sedit c(s) analysis for A1m-L (A), A1m-T (B), S31L-L (C), S31L-T (D), A37L-L (E), A37L-T (F). The protein samples were prepared at 550 μM concentration in 10 mM acetate (pH 4)/100 mM NaCl solution.

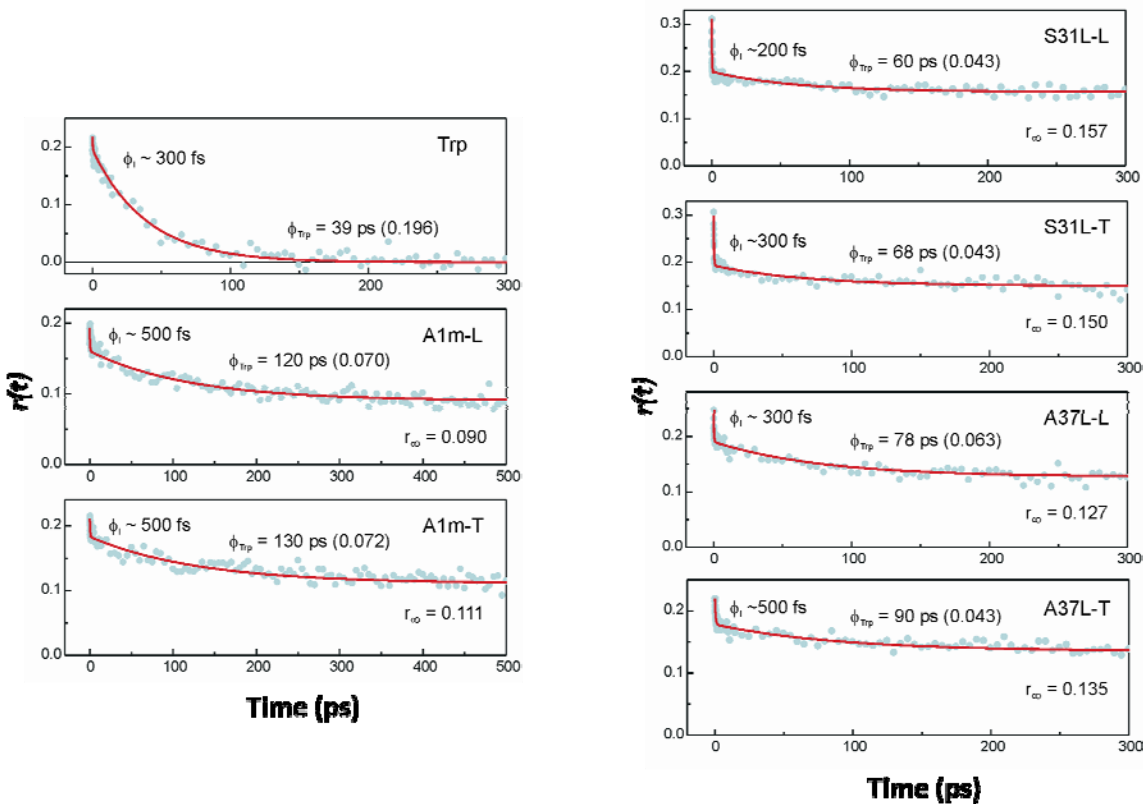

Fig. 3.4. Time-resolved anisotropy, $r(t)$, of the proteins and free Trp. All anisotropy decays were fitted to $r(t) = r_I \exp(-t/\phi_I) + r_{Trp} \exp(-t/\phi_{Trp}) + r_\infty$, where r_I, r_{Trp}, r_∞, ϕ_I, and ϕ_{Trp} are initial ultrafast anisotropy, Trp motion-related anisotropy, offset anisotropy, initial ultrafast internal-conversion time constant of Trp (≤ 500 fs), and Trp-rotational correlation time constant, respectively.

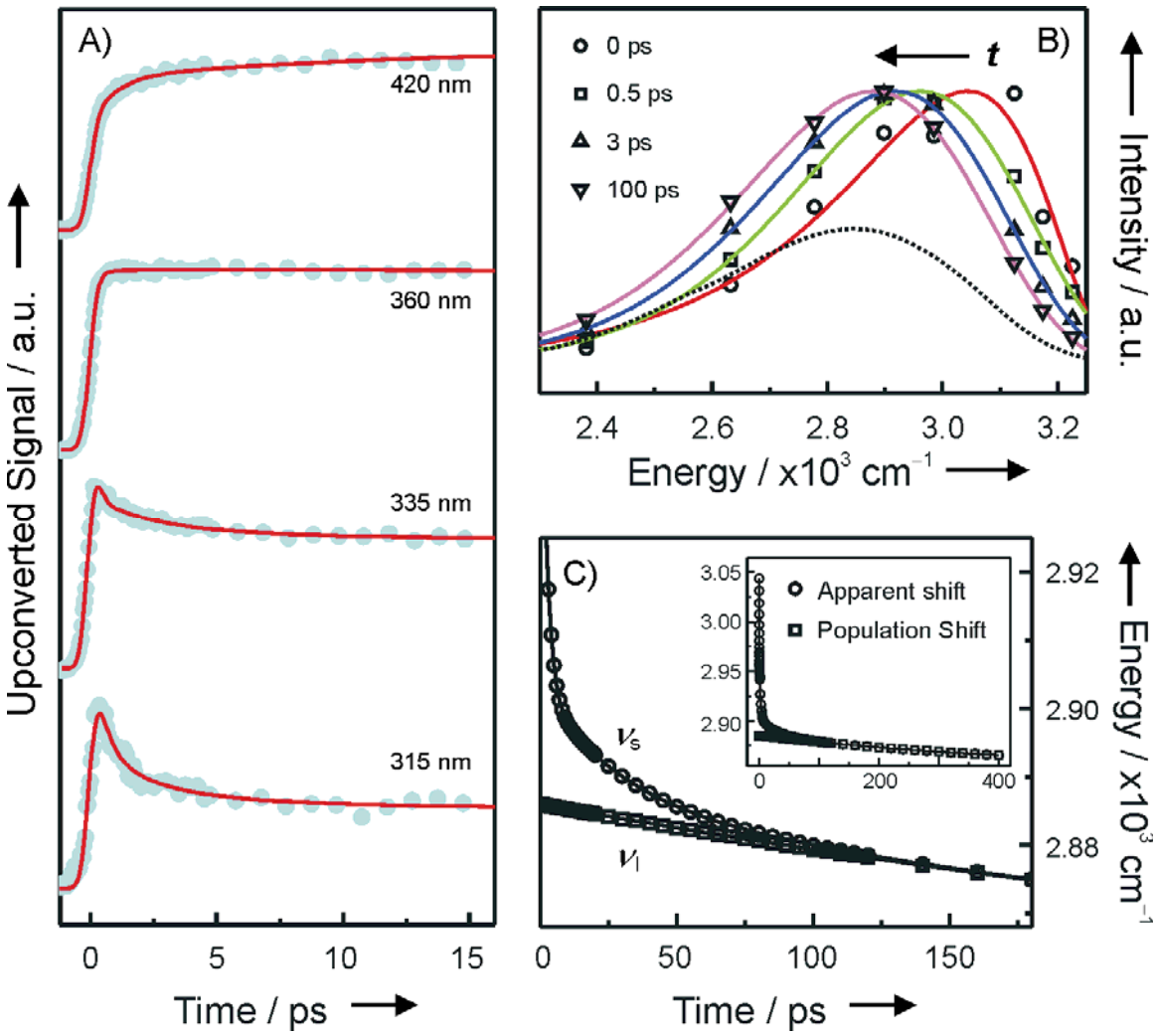

Fig. 3.5. Experimental determination of local hydration dynamics at the surface of the protein A1m-T, excited at 295 nm. A) Representative fs-resolved fluorescence upconversion transients. B) Normalized time-dependent apparent spectral evolution at several time decays. The steady-state emission spectrum is also depicted (dotted line). C) Time-dependent shift of the apparent emission maxima (ν_s) and the lifetime-associated emission maxima (ν_l). Inset: Entire evolution of ν_s and ν_l.

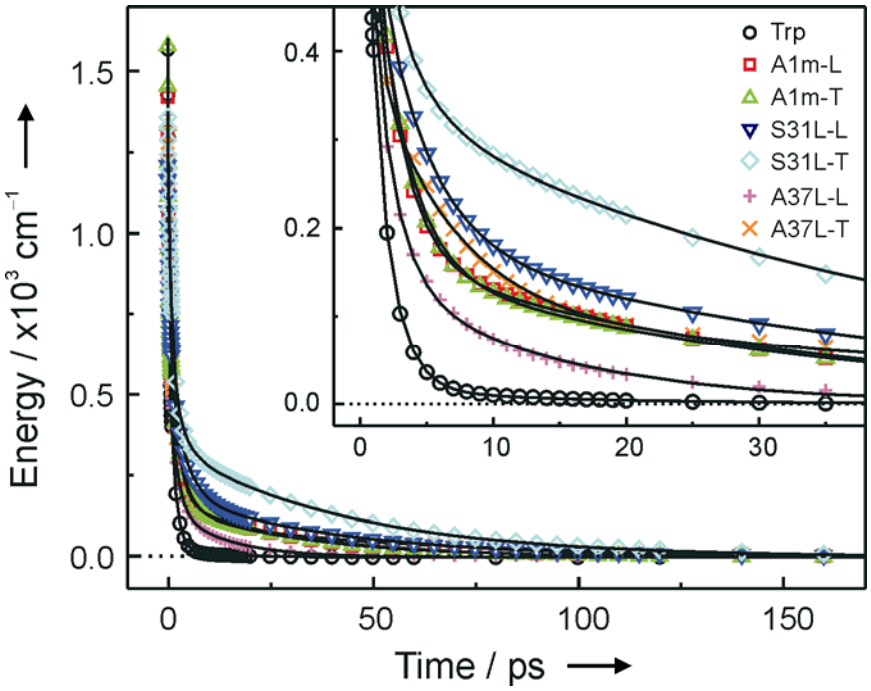

Fig. 3.6. Comparison of the hydration-correlated energy relaxation, $\Delta E_s(t)$, probed by Trp emission. Inset: Enlargement of the early-time hydration behavior. The solvation-energy relaxation of free Trp in the same buffer is also depicted for comparison.

Table 3.1. Fluorescence emission maximum (λ_{max}), hydration-correlated energy relaxation ($\Delta E_s(t)$), and depolarization dynamics ($r(t)$)

Sample	λ_{max} [nm]	$\Delta E_s(t)$[a]						$r(t)$[b]		
		τ_1 [ps]	τ_2 [ps]	τ_3 [ps]	E_1 [cm^{-1}]	E_2 [cm^{-1}]	E_3 [cm^{-1}]	r_{Trp}	ϕ_{Trp} [ps]	θ [^{o}]
Trp	353	0.30	1.5	13	883(0.56)[c]	682(0.43)	18(0.01)	0.196	39	
A1m-L	352	0.30	2.1	31	610(0.43)	646(0.45)	171(0.12)	0.070	120	24
A1m-T	352	0.28	2.5	31	877(0.55)	568(0.35)	161(0.10)	0.072	130	23
S31L-L	349	0.53	3.6	40	580(0.47)	450(0.37)	194(0.16)	0.043	60	16
S31L-T	349	0.79	3.0	48	607(0.46)	375(0.29)	333(0.25)	0.043	68	16
A37L-L	350	0.31	1.7	13	685(0.50)	522(0.38)	157(0.12)	0.063	78	20
A37L-T	349	0.56	6.1	61	871(0.67)	324(0.25)	108(0.08)	0.043	90	17

[a] All hydration-correlated energy relaxation dynamics were fitted to $\Delta E_s(t) = E_1 \exp(-t/\tau_1) + E_2 \exp(-t/\tau_2) + E_3 \exp(-t/\tau_3)$. [b] All anisotropy decays were fitted to $r(t) = r_I \exp(-t/\phi_I) + r_{Trp} \exp(-t/\phi_{Trp}) + r_\infty$, where r_I, r_{Trp}, r_∞, ϕ_I and ϕ_{Trp} are initial ultrafast anisotropy, Trp motion-related anisotropy, offset anisotropy, initial ultrafast internal-conversion time constant of Trp, and Trp-rotational correlation time constant, respectively. The wobbling con semiangles, θ, were extracted with the expression, $1 - r_{Trp}/(r_{Trp} + r_\infty) = [(3\cos^2\theta - 1)/2]^2$. [c] Numbers in parentheses are the fractional amplitude.